Adaptive optics at the PHELIX laser

Hans-Martin Heuck[*a], Ulrich Wittrock[a], Jérôme Fils[b], Stefan Borneis[b], Klaus Witte[b], Udo Eisenbart[b], Dasa Javorkova[b], Vincent Bagnoud[b], Stefan Götte[b], Andreas Tauschwitz[b], Eckehard Onkels[b]

[a]Münster University of Applied Sciences, Stegerwaldstr. 39, 48565 Steinfurt, Germany
[b]GSI: Gesellschaft für Schwerionenforschung mbH, Planckstr. 1, 64291 Darmstadt, Germany.

ABSTRACT

GSI Darmstadt currently builds a high-energy petawatt Nd:glass laser system, called PHELIX (Petawatt High-Energy Laser for Heavy-Ion Experiments). PHELIX will offer the world-wide unique combination of a high-current, high-energy heavy-ion beam with an intense laser beam. Aberrations due to the beam transport and due to the amplification process limit the focusability and the intensity at the target. We have investigated the aberrations of the different amplification stages. The pre-amplifier stage consists of three rod-amplifiers which cause mainly defocus, but also a small part of coma and astigmatism. The main amplifier consists of five disk amplifiers with a clear aperture of 315 mm. These large disk-amplifiers cause pump-shot aberrations which occur instantly. After a shot, the disk amplifiers need a cooling time of several hours to relax to their initial state. This limits the repetition rate and causes long-term aberrations. We will present first measurements of the pump-shot and long-term aberrations caused by the pre- and the main amplifier in a single-pass configuration. In this context, we will present the adaptive optics system which is implemented in the PHELIX beam line and discuss its capability to compensate for the pump-shot and long-term aberrations.

Keywords: adaptive optics, high-energy laser, petawatt laser

1. INTRODUCTION

PHELIX is projected for the peak power of one petawatt (1 PW = 10^{15} Watt). It is being built at the Gesellschaft für Schwerionenforschung (GSI) in Darmstadt. After its completion, PHELIX can operate in the high-peak power configuration with a pulse energy of up to 500 J and a pulse duration of 500 fs or in the high-energy configuration with a pulse energy of up to 1000 J at the pulse duration of 10 ns.[1]

The GSI performs basic and applied research in physics using heavy ion accelerators. With the heavy-ion accelerator all elements can be accelerated up to 2 GeV per mass unit. The key of main interest are nuclear and hadron physics, atom physics and plasma physics. The PHELIX laser will allow new experiments based on the symbiotic use of an intense heavy-ion beam and a high-energy laser. In the latter field, the investigation focus on warm dens matter (WDM). This state is achieved by quasi-isochronic heating of solids up to a few eV using the heavy-ion beam. The purpose of PHELIX is to act as a backlighter source of hard X-rays which diagnose the interior of the heated sample.[2] The realization of pulses with a high-peak power in excess of 1 PW = 10^{15} Watt has been enabled by the invention of chirped pulse amplification (CPA).[3] Based on this scheme, several peta-watt-class laser systems have been built or are currently under construction.[4] These high-intensity laser systems have opened the path to new phenomena like the acceleration of high-energy particle beams or the exploration of relativistic plasma physics.[5–8] With the CPA technique, a short laser pulse is temporarily stretched by a factor of 10^4 before amplifying it up to the desired pulse energy. This way, the peak intensity in the laser system during amplification remains low enough to avoid damage of optical components and pulse distortion due to non-linear effects. Finally, the energetic pulse is compressed to a pulse duration close to the original value. In Nd:glass lasers this is typical 500 fs.

The experiments mentioned above either require a high fluence or high intensity. Spatial phase aberrations enlarge the focal spot diameter and therefore reduce the fluence and intensity of the laser pulse. The reasons for spatial phase aberrations in an amplification chain are manifold. E. g. spatial aberrations result from unachievable perfections of optical components like mirrors, lenses, beam splitter, polarizers or compromises in the optical set-up. However, the largest portion of spatial aberrations results from thermo-optical aberrations. By knowledge of the static and thermo-optical aberrations, the distorted intensity pattern in the focal spot can be predicted and thus, the requirements that have to be met by adaptive optics for the correction of these aberrations can be specified. Adaptive optics allow for compensation of aberrations. First experiments with an adaptive optics system were reported in the nineties on the NOVA petawatt chain.[9]

An adaptive mirror with an actively controlled surface is placed in the PHELIX beamline. Currently, the mirror control signal is directly calculated out of a wavefront measurement. With this closed-loop system, the compensation of thermo-optical aberrations at PHELIX was demonstrated. Within the scope of this paper, the source of static and thermo-optic aberrations are investigated and the adaptive closed-loop system will be presented.

2. THE PHELIX LASER SYSTEM

Following the closure of the high-energy lasers PHEBUS in France and the NOVA laser at the Lawrence Livermore National Laboratory (LLNL)[10] some of the beam lines were passed on to several research facilities around the world, e. g. the Vulcan laser facility in Great Britain and the LULI in France.[11,12] Also the PHELIX laser is built from these components.[13]

PHELIX consists of two independent oscillators with amplifier stages, called front-ends, where pulses are generated and amplified up to a common energy level of 50 mJ with a repetition rate of 10 Hz. In the high-
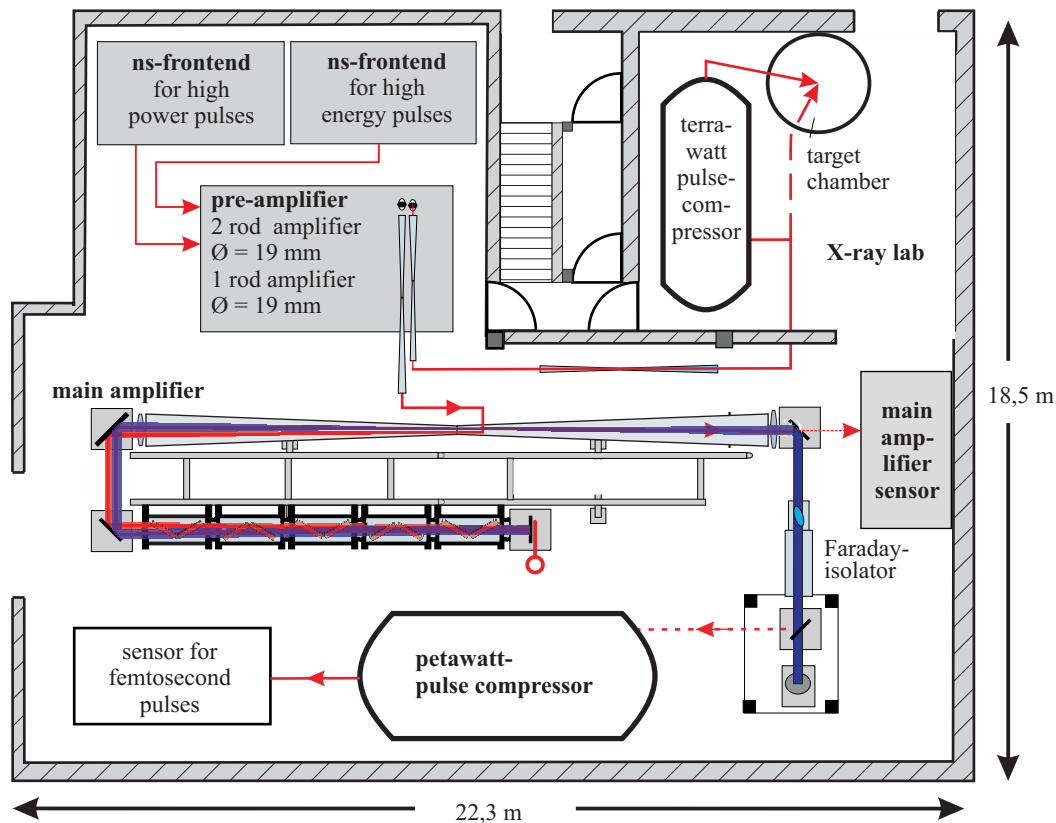

Figure 1. Schematic layout of the PHELIX laser.

Figure 2. a) A total of 340 capacitors have been installed. b) Installation and alignment of the double-pass section of the main amplifier.

energy configuration, the pulses are generated by a fiber-oscillator with a pulse duration from 1 to 20 ns with a programmable pulse shape. This ns-front-end is a slightly modified copy of the front-end prototype of the National Ignition Facility (NIF, USA).[10] In the high-power configuration, a femtosecond Ti:sapphire oscillator running at a wavelength of 1053 nm generates pulses with a duration of 100 fs. The pulses are stretched with a grating stretcher to a pulse duration of 2 ns before they are amplified in two Ti:sapphire regenerative amplifiers.[14] This fs-front-end is a copy of the original NOVA petawatt front-end.[15]

Selected pulses from one or the other front-end is passed to the pre-amplifier section. Here, the pulses are amplified in a single passage through two 19-mm and one 45-mm diameter Nd:glass rods, all pumped by flash lamps. At the entrance of the pre-amplifier a serrated aperture[16] defines an object plane which is magnified and relay-imaged on to the rod mid planes and in the end of the pre-amplifier on a bimorph adaptive mirror. This adaptive mirror has a clear aperture diameter of 65 mm. Five vacuum telescopes are employed for magnification of the beam, relay imaging and spatial filtering. During the whole amplification process, the beam size is expanded to reduce the fluence on the optic and to reduce nonlinear effects.

The following main amplifier is capable to amplify pulses from the pre-amplifier up to 1 kJ in the high-energy configuration. In the high-power configuration, the main amplifier amplifies the stretched pulses up to an energy of 500 J before a grating compressor will re-compress them to a pulse duration of 500 fs. Thus, the pulses reach peak powers in the order of 1 Petawatt. In the main amplifier, the pulses are expanded to a diameter of 250 mm. The main amplifier is a double-pass amplifier and consists out of ten flash lamp-pumped disks. The pulse from the pre-amplifier is injected through a pinhole in the center of a 15 m long 1:1telescope. Separation of the injected and the amplified beam is realized by a second pinhole in the telescope focal plane and a slight tilt of the injection and retro-reflecting mirror. One of the mirror holders in the main amplification chain, the retro-reflecting mirror holder, was modified following a proposal from Hernandez[17] to deform the mirror and to pre-correct for astigmatism.

The entire laser system is embedded inside a 18 x 22 m^2 two-storey building. The ground floor is a class 10000 clean room and houses the optical set-up, see Fig. 1, while the 2nd floor comprises the high-voltage switches and capacitor banks, a class 100 clean room for handling of sensitive optics and the main control room. Figure 2 shows the capacitor room with a total of 340 capacitors and the double-pass section of the main amplifier. The pulses are transported from the laserlab with telescopes outside the laser building to the the experimental areas of the ion-accelerator.

PHELIX is currently under construction. All data presented in this paper are measured in a single-pass configuration of the main amplifier. In the single pass configuration, the beam was analyzed after a single passage through the main amplifier at the position of the retro reflecting mirror.

3. MOTIVATION FOR ADAPTIVE OPTICS

Realizing very high-energy and very high-power is one of the major challenges of this laser project. The output power is limited by the energy fluence on the surface or inside the optical components. If we want to increase the energy, we need to expand the beam diameter. To realize this, bigger and much more expensive amplifier disks, mirrors, gratings, and so on are required. On the other hand, the beam quality is limited by wavefront aberrations which limit the achievable intensity and fluence in the focal spot. If we are able to increase the beam quality we get a higher brightness and consequently more energy and power onto the target.

The Strehl-ratio employed by K. Strehl[18] is a commonly used approximation to calculate the intensity decrease caused by small wavefront aberrations. The Strehl-ratio is defined as the ratio between the peak intensity of an image of a point source with and without aberrations.

Similar to the original definition we define the Strehl-ratio as the ratio between the measured peak intensity of a pulse in the focal plane of a lens and the diffraction-limited peak intensity with the same intensity distribution in the near field. The Strehl-ratio is defined for a uniform intensity distribution in the near field and does not allow disturbance in the near field intensity pattern. The PHELIX laser has a nearly top-hat like intensity distribution. Therefore, the Strehl-ratio offers a possibility to estimate the influence of aberrations in the focal plane. Generally, the Strehl-ratio is not a good number to quantify the beam quality of a laser because the intensity distribution in the near field is not considered.[19]

The Strehl-ration S can be approximated from rms-wavefront error σ and the wavelength of the laser λ:[20]

$$S = 1 - \left(\frac{2\pi}{\lambda}\right)^2 \sigma^2. \tag{1}$$

This approximation is valid for ratios greater than 0.5. According to the Maréchal-criterion, an optical system or a laser beam is said to be diffration-limited if the Strehl-ratio is greater than 0.8. With eq. (1) a laserbeam is diffration-limited if the rms-wavefront error is less than $\lambda/14$. Mostly, we deal with large wavefront errors and Strehl-ratios smaller than 0.5. A better approximation for ratios larger than 0.1 was given by Graham:[21]

$$S = \exp\left[-\left(\frac{2\pi}{\lambda}\right)^2 \sigma^2\right]. \tag{2}$$

Both equations allow an estimation of the influence of wavefront aberrations on the peak intensity. For example, if the rms-wavefront is around $\lambda/8$ the intensity is reduced by a factor of 2 and with an rms-wavefront of $\lambda/4$ the intensity is reduced by a factor of 10. These numbers show the importance of a good wavefront quality. We will see in the next section that aberrations at PHELIX are large and reduce the intensity significantly.

4. ABERRATION SOURCES AT PHELIX

4.1. Static aberrations

A geometric-optical calculation shows that the whole amplification chain of the pre- and main amplifier has an aberration with a peak-to-valley (pv-)difference of 0.9 λ, shown in Fig. 3.a. The static aberrations mainly consist of spherical aberration (Zernike coefficient $a_8 = 0.4$) and astigmatism ($a_4 = 0.26$), measured at the PHELIX wavelength of 1053 nm. Astigmatism results from tilted lenses. It is necessary to tilt the lenses in the telescopes of the main and pre-amplifier to reflect ghost foci out of the beam line.[22]

Beside these tolerated failures in the optical design, surface or bulk errors of optical components are a second reason for static aberrations. Typical laser optics are specified with a pv-aberration below $\lambda/10 - \lambda/20$. At PHELIX, all optics smaller than 100 mm are specified with a pv-aberration below $\lambda/10$. But for larger optics it gets more and more cost intensive to produce such precise large optics. As a compromise between a good surface quality and costs we define larger optics with a pv-difference between $\lambda/3$ and $\lambda/10$. How sensitive large optics is to an external influence shows Fig. 3.b. The picture shows the wavefront map of a turning mirror from the main amplifier with diameter of 520 mm. Wavelength in this measurement was 633 nm with an angle of incidence is 45° degrees to the surface. Although – in this example – the mechanical stress of the coating was considered, the pv-wavefront aberration after coating of the mirror is 0.3 λ, before it was 0.1 λ. Also mechanical stress from the mirror holder can deform such a large mirror easily.
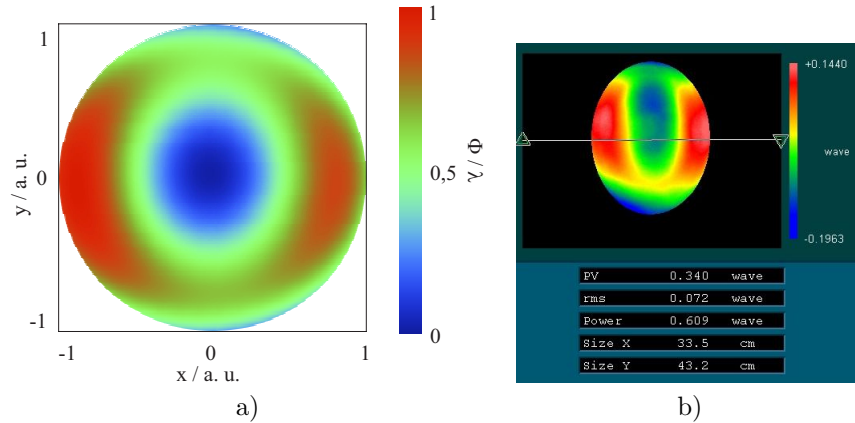
Figure 3. a) Calculated wavefront error from the pre-amplifier to the end of the main amplifier. b) Measured surface of one of the 45° turning mirrors after coating.

4.2. Thermo-optical aberrations

The optical pumping of solid state lasers is always coupled with a strong heat generation. Heat modifies the mechanical and optical properties of the pumped media, e. g. the refractive index or the mechanical length which induce a mechanical stress inside the media. Again, stress leads to a change of the refractive index.

Provided the ideal case, the active media in high-energy and ultra high-power lasers is completely cooled down between shots. However, a part of the thermo-optical aberration occurs before the laser pulse is amplified. Relaxation from the pump state to the higher laser state immediately raises heat generation. Additionally, the flash lamps emit a part of the light in the UV-regime which is absorbed on the surface of laser glass.

After a shot, the active media and all other components which are heated by the flash lamps have to cool down. From NOVA it is reported that the 315 mm-disk amplifiers have a very long relaxation time,[9] so that a repetition rate of the main amplifier of 1 shot in two hours seamed to be realistic in the PHELIX proposal.

We differentiate two impacts of thermo-optical aberrations on the laser chain. The optical pumping immediately induces a temperature profile within the rods and disks which causes the *pump-shot* aberrations. After a shot, the amplifiers must cool down. The air-cooled disc amplifiers inside the main amplifier need several hours to fully relax to their initial state. The aberrations which arise during the cooling are named *long-term* aberrations.

4.2.1. Pump-shot aberrations

In the pre-amplifier the flash lamps are placed in a radial-symmetric geometry around the laser rods. The pump light is absorbed exponentially, according to Beer's law. In a first approximation and due to the large optical bandwidth of the pump light, the temperature profile is approximately hyperbolic which leads to a thermal lens. Figure 4 shows the pump-shot aberrations of the pre- and main amplifier. The rod amplifiers produce a thermal lens with a pv-aberration of 0.6 μm ($a_3 = 0.3$). But coma with a pv-aberration of 0.1 μm and astigmatism with a pv-value of 0.2 μm is unusual for rod amplifiers with radial symmetry.

In the main amplifier the flash lamps are placed left- and right-hand of the disc surfaces, see Fig. 5.a). In the ideal case the flash lamp light is absorbed homogeneously over the surface and exponentially in the depth of the disk. As long as the heat deposition is homogeneous over the surface, aberrations should not occur. But around the laser disks with an octagon shape a cladding absorbs the spontaneous emission. A sketch of an octagon-laser disk is drawn in Fig. 5.b. This avoids parasitic lasing inside the disks. The disadvantage is that the temperature of the cladding increases by an average of 1.5 °C due to absorption of spontaneous emission. Also the absorption inside the cladding follows Beer's law. Pitts[23] reports for the same type of laser disks, that the boundary layer between glass and cladding heats up to 40 °C. The thermal load produce a mechanical stress and shock waves which affect the transmitted wavefront of the laser beam instantly.
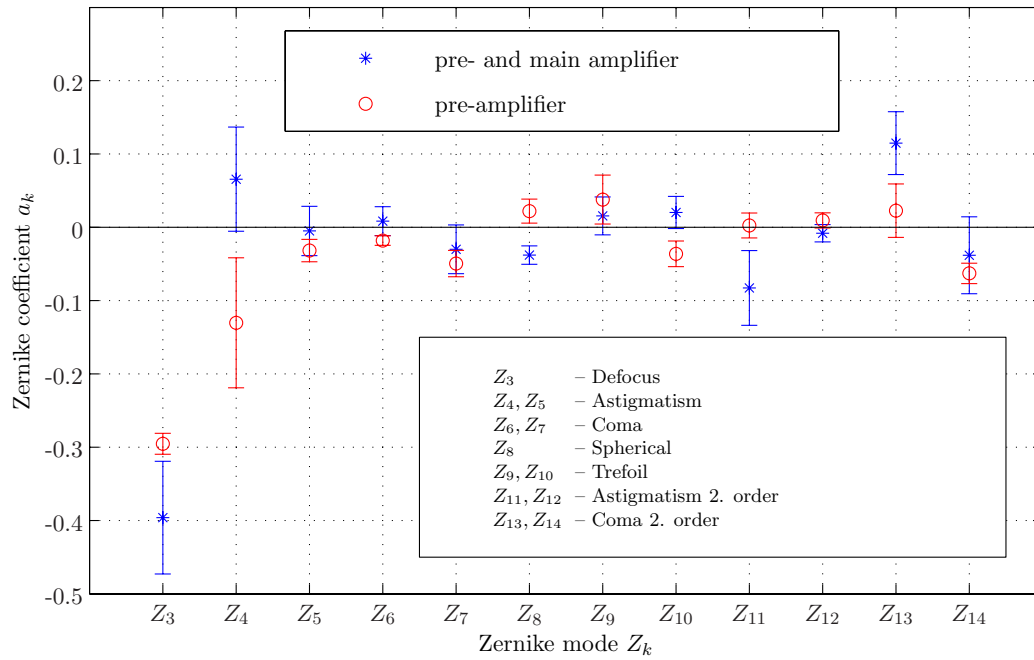
Figure 4. Comparison between pre-amplifier and main amplifier pump-shot aberrations.
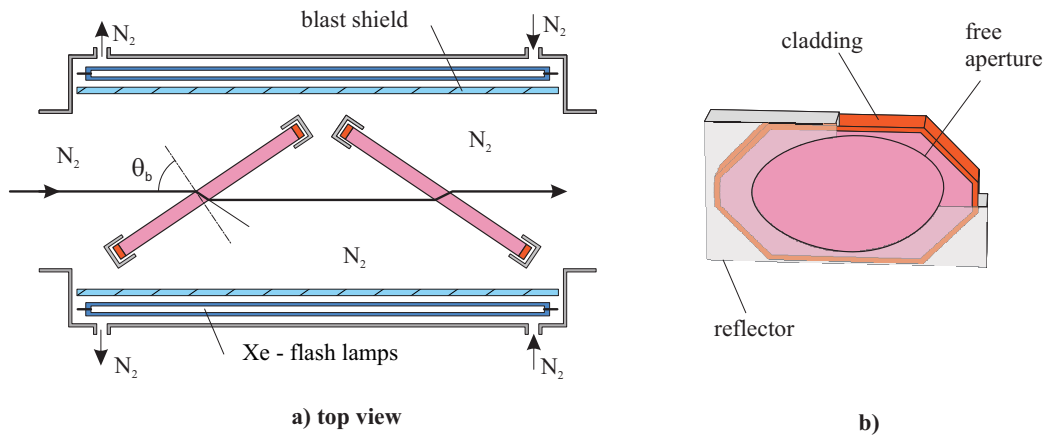

a) top view

b)

Figure 5. a) Scheme of a disk amplifier with two Nd:glass amplifiers disks. b) Nd:glass disk with bonded cladding and reflector to protect the cladding from the flash lamp light.
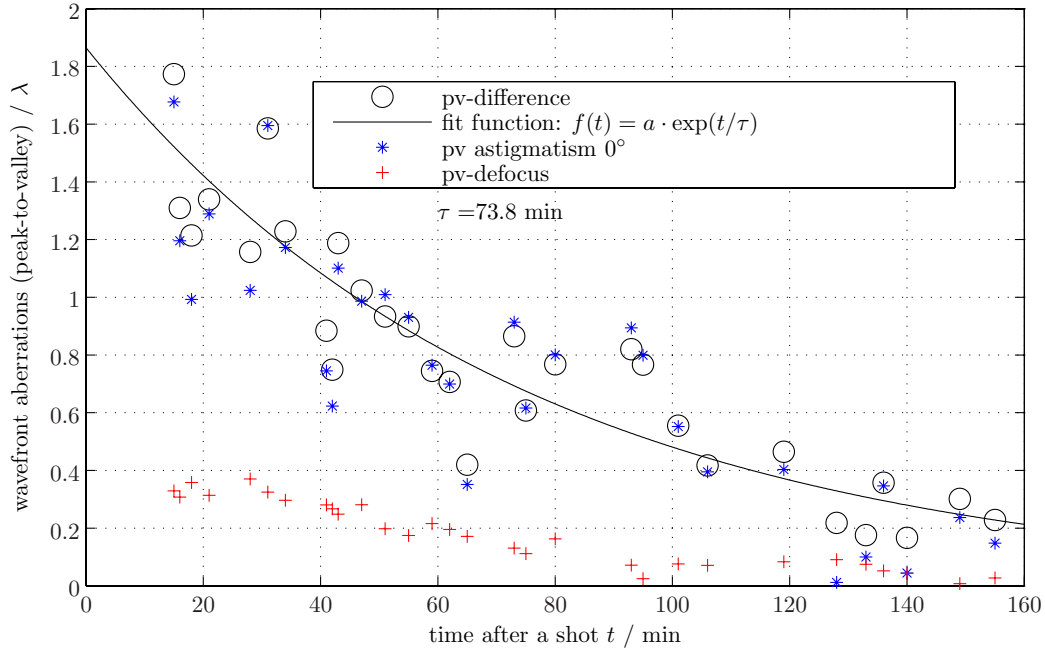
Figure 6. Long-term aberration of the main amplifier over time after a shot.

To measure the pump-shot aberrations of the main amplifier, a series of shots every 3 hours with the same laser parameters (main amplifier energy input of 5 J, main amplifier gain of 10, etc.) was analyzed. To separate the influence of the pre-amplifier from that of the main amplifier we had to measure the wavefront in front of and behind the main amplifier in two different series. Both measurements are plotted in Fig. 4. The main amplifier introduces mainly astigmatism, second-order astigmatism and second-order coma along the principle axis of the discs. Defocus is mainly caused by the pre-amplifier. The magnitude of defocus and astigmatism is predictable and correctable with a static deformable mirror and a movable lens.[24]

4.2.2. Long-term aberrations

While the water-cooled rod amplifiers of the pre-amplifier are cooled down in a few minutes, the main amplifier is cooled by dry nitrogen at atmospheric pressure and temperature. A FEM calculation shows, that due to the high heat capacity and low heat conductivity, the huge glass volume needs more than two hours to cool down – two hours was the planned repetition rate in the PHELIX proposal. During the cooling, a temperature profile is built inside the laser disks. However, if we calculate the worst-case scenario that all electric pump energy goes completely inside the laser discs and builds up a laterally strong thermal profile, we can only state a pv-deformation of a few hundred nanometers.[24] Another explanation for aberrations caused by a thermal load in the disks was given by Murray.[25] If the disks are heated up or cooled inhomogeneously, they will bend. This will cause aberrations due to the thickness of the disks. Moreover, the mirrors close to the amplifiers can heat up inhomogeneously, too, and deform spherically. Under 45° degree angle of incidence a spherical deformation of a turning mirror results in astigmatism.

The long-term aberrations were measured every five minutes with the alignment beam after firing once. The pv-aberrations are shown in Fig. 6. Ten minutes after a shot, the aberrations had grown up to two wavelengths and fell down exponentially in three hours to a value below $\lambda/5$. To characterize the cooling time with a single number we have fit an exponential decay (line) on the pv-abberations (circles):

$$f(t) = b \cdot \exp(-\frac{t}{\tau_h}). \tag{3}$$

The fit-function $f(t)$ determines the time τ_h, after which the aberrations fall down to $1/\mathrm{e} = 37\,\%$. Here b is the pv-aberration at $t = 0$. In this example the characteristic cooling time is 73.8 minutes. Figure 6 also shows
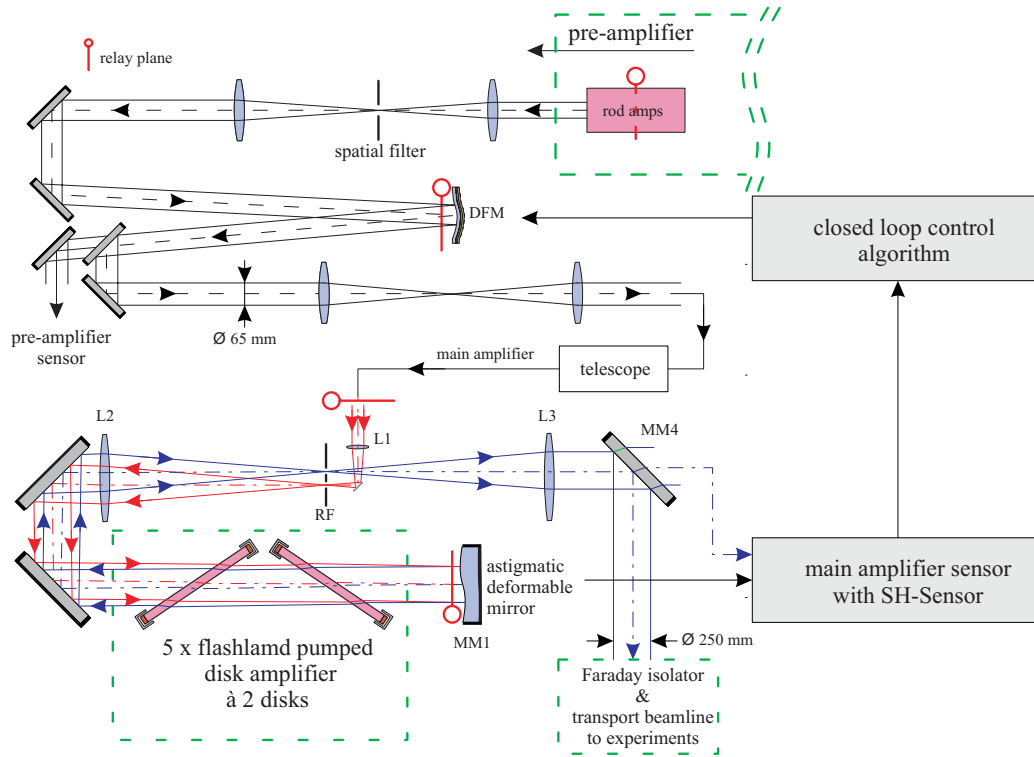
Figure 7. Optical set-up to compensate for long-term aberrations. The rod mid-planes inside the pre-amplifier are imaged onto the bimorph mirror. This image plane is relayed with telescopes inside the main amplifier section. The wavefront is measured with a SH-sensor in the single-pass set-up behind mirror MM1. In the final set-up in the wavefront is measured behind MM4.

the portion of defocus (cross) and astigmatism (stars). The largest contribution to the aberrations are due to astigmatism and defocus. Defocus falls down to its original state in 60 minutes but astigmatism is present during the whole cooling period. These huge and strongly fluctuating aberrations limit the repetition rate of PHELIX to one shot in three hours.

5. ADAPTIVE OPTICS

To correct the aberrations described above we have implemented two adaptive mirrors in the PHELIX laser – an actively controlled bimorph mirror bought from company NightN Ltd and a static deformable HR-mirror in the main amplifier.

The static deformable mirror is a conventional HR-coated mirror. On the outer ring of the mirror screws can deform the mirror to an astigmatic shape.[17, 26] The screws are currently not controlled by a closed-loop. The shape should be optimized once after characterizing the main amplifier. In this meaning, this mirror is a static mirror. The bimorph adaptive mirror consists of a dielectric coated glass substrate that is attached with its backside to a stack of two piezo disks. The piezo disks themselves are coated with 31 copper electrodes. The maximum achievable deformation of this mirror is about 6λ. This mirror is placed at the exit of the pre-amplifier in an image plane of the pre-amplifier rods, see Fig. 7. This image is relayed with telescopes in the middle of the main amplifier. After the main amplifier mirror 4 (MM4), a portion of the pulse (1.5 %) is transmitted into the diagnostic section. Here, the wavefront is measured with a Shack-Hartmann(SH)-Sensor and is characterized here for example by the Zernike coefficients a_k which are grouped in a vector $\vec{a}$. However, the algorithm works also with spot displacements of a Shack-Hartmann pattern or other measures which describes the wavefront. The wavefront $\Phi(x,y)$ can be reconstructed with the Zernike polynominals Z_k grouped in a vector $\vec{Z}$, where k is the order of the polynominals.

$$\Phi(x, y) = \vec{a} \cdot \vec{Z}(x, y). \tag{4}$$

5.1. The control loop

As a first step to install the closed-loop, the SH-sensor had to be calibrated with a plane wavefront. A diffraction-limited pinhole was installed in front of the wavefront sensor into the last telescope to produce a plane wavefront. In the next step, the response of the mirror surface to an applied voltage at each individual mirror electrode had to be recorded. These responses can be described by the so-called influence functions.[27] This set of functions is grouped into the influence function matrix B. Assuming that the process is linear, one obtains the Zernike coefficients of the deformed mirror surface $\vec{a}_{\mathrm{dm}}$ as the response to a given voltage vector $\vec{x}$:

$$\vec{a}_{\mathrm{dm}} = \mathbf{B} \cdot \vec{x}. \tag{5}$$

Measuring the wavefront with the Shack-Hartmann sensor in the close-loop, the required voltages are calculated for the inverse mirror surface by inverting of eq. (5)

$$.\vec{x} = \mathbf{B}^{-1} \vec{a}_{\mathrm{dm}}. \tag{6}$$

As the matrix B is generally not square and the non-singularity of the matrix can not be guaranteed, the pseudo-inversion of the matrix M is built with the singular-value decomposing method (SVD).[28] The SVD is useful because the the eigen-modes respectively the singular-modes of the mirror surface can be obtained and any surface can be described by a linear combination of these modes. This allows to compute the surface which is the best approximation to the desired surface.[26]

5.2. The PHELIX adaptive optics system

As described in the last section we have two families of actuators to manipulate the spatial phase:

- $\vec{a}_{\mathrm{dm}}$ – the Zernike coefficient vector of the spatial phase of the bimorph deformable mirror.

- $\vec{a}_{\mathrm{sm}}$ – the Zernike coefficient vector of the spatial phase of the static deformable mirror.

And three sources of aberrations in the laser chain:

- $\vec{a}_{\mathrm{s}}$ - the Zernike-coefficient vector of static aberrations of the laser chain.

- $\vec{a}_{\mathrm{ps}}$ - the Zernike-coefficient vector of pump-shot aberrations of both, the pre- and main amplifier.

- $\vec{a}_{\mathrm{lt}}(t)$ - the Zernike-coefficient vector of long-term aberrations of the main amplifier, which depend on the cooling time t.

In a first step, we have tried to compensate for the long-term aberrations of the main amplifier in a single passage without the static deformable mirror. For this experiment, the SH-sensor was calibrated to an external point source and not to the beam line. By this way, the static aberrations of the laser chain and additionally those of the diagnostic unit were compensated by the closed-loop. As the static aberrations of the diagnostic unit are quite small (pv-aberration $\leq \lambda/4$) they are negligible. With eq. (6), the control signal for the bimorph mirror can be calculated out of a wavefront measurement which is described by the Zernike-coefficients a_d:

$$.\vec{x} = -B^{-1}(\vec{a}_{\mathrm{d}} - \vec{a}_{\mathrm{dm}}) = -B^{-1}(\vec{a}_{\mathrm{s}} + \vec{a}_{\mathrm{s}} - \vec{a}_{\mathrm{dm}}). \tag{7}$$

a_d is the sum out of the static and long-term aberrations and the mirror surface of the bimorph mirror $\vec{a}_{\mathrm{dm}}$ during the measurement. After a shot, an alignment beam was feed through the laser chain to measure the long-term aberrations. If the aberrations are weak and stable enough to be compensated by the adaptive mirror, the laser chain has to be switched back to the shot mode. To avoid an unstable state of the mirror surface, the
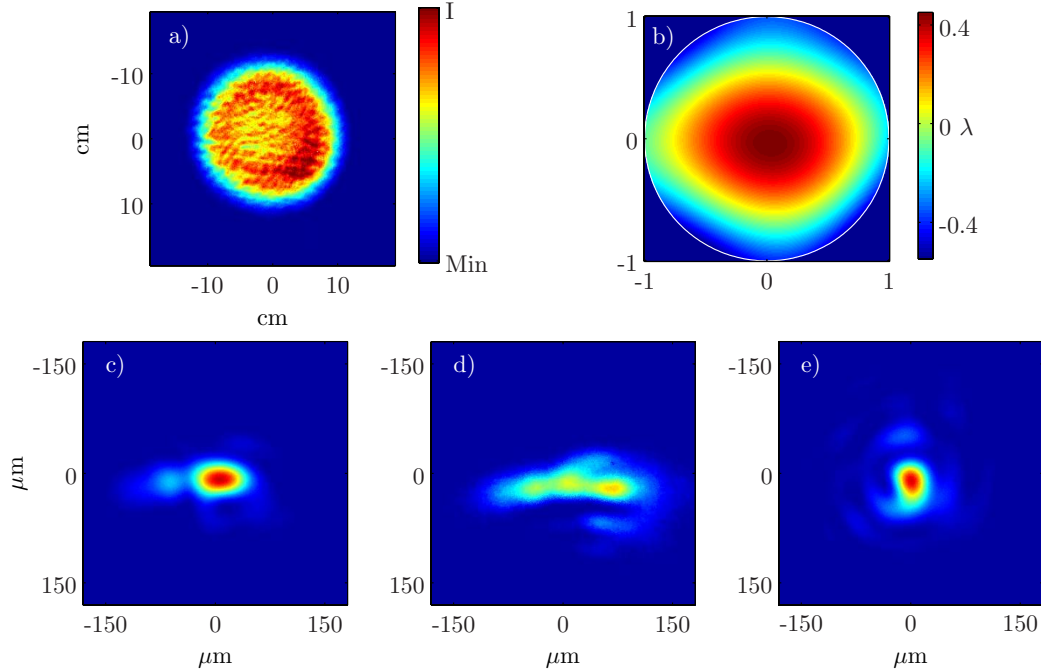
Figure 8. a) and c) Near field and far field fluence patterns and b) wavefront map of the near field of a main amplifier shot. The main amplifier was completely cooled down. Patterns d) and e) show the far field shot only 1h54 and 1h19 after firing the main amplifier, respectively. In e) the long-term aberrations are pre-compensated by the bimorph deformable mirror.

close-loop is interrupted and the surface of the bimorph mirror is frozen. Hence, the long-term aberrations have to be stable over a period of at least five minutes – the time to switch between these two operation modes.

Figure 8 shows the results of the compensation for the long-term aberrations arising from the main amplifier. All shots of the main amplifier had an output energy of around 50 J. In a) and c) the near and far field fluence pattern from a thermally unloaded shot is plotted, b) shows the wavefront map of the near field. We shot again after 1h54 and saw a strongly distorted far field pattern, shown in Fig. 8.d). With the closed-loop system we could compensate the long-term aberrations after a cooling time of 1h19. As the bimorph mirror also reduces the static aberrations, the far field pattern in e) is slightly better than the thermally unloaded far field in c).

To compensate for pump-shot aberrations, these aberrations have to be measured in a main amplifier shot when the system is thermally unloaded. They have to be considered in the calculation of the closed-loop system:

$$\vec{x} = -B^{-1}(\vec{a}_{\mathrm{s}} + \vec{a}_{\mathrm{s}} + \vec{a}_{\mathrm{s}} - \vec{a}_{\mathrm{dm}}). \tag{8}$$

This has not been realized yet and will be done in the near future.

6. SUMMARY AND OUTLOOK

The performance of the PHELIX laser is limited by spatial phase aberrations. They reduce the brightness and limit the repetition rate. In this paper, the static and thermo-optical aberrations were analyzed and adaptive optics were used to compensate them. The correction of the aberrations occurring after a shot increases the repetition rate of PHELIX from 1 shot in 3 hours to 1 shot in 1h19 with an additional increase of the brightness by compensating static aberrations.

The double-pass section of the main amplifier was finished in March 2007 and first preliminary experiments were done. All measurements presented in this paper were carried out in a single-pass configuration through the main amplifier. They are currently repeated and the final adaptive optics closed-loop system to compensate

for the long-term aberrations will be installed soon. Additionally, the static deformable mirror can help to compensate for pump-shot and long-term aberrations. The next major milestone will be the extention of the closed-loop system to correct for long-term and pump-shot aberrations simultaneously.

REFERENCES

1. T. Kühl and J. Kluge, et al., "PHELIX proposal part b," Tech. Rep. http://www-aix.gsi.de/phelix/, GSI, 1998.
2. T. Kühl and J. Kluge, et al., "PHELIX proposal part a," Tech. Rep. http://www-aix.gsi.de/phelix/, GSI, 1998.
3. D. Strickland and G. A. Mourou, "Chirped pulse amplification," *Opt. Commun.* **55**, p. 219, 1985.
4. J. D. Zuegel, S. Borneis, C. Barty, B. LeGarrec, C. Danson, N. Miyanaga, K. Rambo, P. C. LeBlanc, J. Kessler, T. A. Schmid, L. J. Waxer, J. H. Kelly, B. Kruschwitz, R. Jungquist, E. Moses, J. A. Britten, I. Jovanovic, J. Dawson, and N. Blanchot, "Laser challenges for fast ignition," *Fusion Sci. Technol.* **49**, pp. 453–482, April 2005.
5. K. Ledingham, P. McKenna, and R. Singhal, "Applications for nuclear phenomena generated by ultra-intense lasers," *science* **300**(5622), pp. 1107–1111, 2003.
6. S. P. D. Mangles, C. Murphy, Z. Najmudin, A. Thomas, J. Collier, A. Dangor, E. Divall, P. Foster, J. Gallacher, C. Hooker, D. Jaroszynski, A. J. Langley, W. B. Mori, P. A. Norreys, F. S. Tsung, R. Viskup, B. R. Walton, and K. Krushelnick, "Monoenergetic beams of relativistic electrons from intense laser- plasma interactions," *Nature* **431**, pp. 535–538, 2004.
7. C. G. R. Geddes, C. Toth, J. van Tilborg, E. Esarey, C. B. Schroeder, D. Bruhwiler, C. Nieter, J. Cary, and W. P. Leemans, "High-quality electron beams from a laser wakefield accelerator using plasma-channel guiding," *Nature* **431**, pp. 538–541, Sept. 2004.
8. J. Faure, Y. Glinec, A. Pukhov, S. Kiselev, S. Gordienko, E. Lefebvre, J.-P. Rousseau, F. Burgy, and V. Malka, "A laser-plasma accelerator producing monoenergetic electron beams," *Nature* **431**, pp. 541–544, Sept. 2004.
9. T. Cowan, B. Hammel, S. Hatchett, E. Henry, M. Key, J. Kilkenny, J. Koch, A. Langdon, B. Lasinski, and R. Lee, "Progress in fast ignitor research with the nova petawatt laser facility," in *Proceeding of 17th International Atomic Energy Agency Fusion Energy Conference, Yokohama (JP)*, 1998.
10. Lawrence Livermore National Laboratory, 7000 East Ave., Livermore, CA 94550-9234. http://www.llnl.gov/str/Remington.html.
11. Central Laser Facility Rutherford Appleton Laboratory (CLF), Chilton, Didcot, Oxfordshire, OX11 0QX. http://www.clf.rl.ac.uk/.
12. LULI, Palaiseau, France. http://www.luli.polytechnique.fr/.
13. Gesellschaft für Schwerionenforschung mbH, Planckstr. 1 64291 Darmstadt. http://www.gsi.de/phelix.
14. D. Javorkova, P. Neumayer, T. Kühl, S. Borneis, E. Brambrink, C. Bruske, E. W. Gaul, S. Götte, T. Hahn, H.-M. Heuck, *et al.*, "New PW stretcher-compressor design for PHELIX laser," in *Proceedings of the SPIE*, **5945**, pp. 350–360, 2005.
15. M. D. Perry, D. M. Pennington, B. C. Stuart, G. Tietbohl, J. A. Britten, C. Brown, S. Herman, B. Golick, M. Kartz, J. Miller, H. T. Powell, M. Vergino, and V. Yanovsky, "Petawatt laser pulses," *Opt. Lett.* **24**, pp. 160–162, February 1999.
16. J. Auerbach and V. Karpenko, "Serrated-aperture apodizers for high-energy laser systems," *Appl. Opt.* **33**, pp. 3179–3183, 1993.
17. C. Hernandez-Gomez, J. Collier, and S. Hawkes, "Vulcan intensity increase by wavefront quality improvement," tech. rep., CLRC Rutherford Appleton Laboratory, Chilton, Didcot, Oxon OX11 0QX, 1997.
18. K. Strehl, "Aplanatische und fehlerhafte abbildung im fernrohr," *Zeitschrift für Instrumentenkunde* **15**, pp. 362–370, 1895.
19. E. Siegman, A. "How to (maybe) measure laser beam quality," *DPSS Lasers: Applications and Issues (OSA TOPS Volume 17)* **17**, pp. 184–199, 1998.
20. M. Born and E. Wolf, *Principles of optics : electromagnetic theory of propagation, interference and diffraction of light*, Pergamon Press, Oxford [u.a.], 6. (corr.) ed., reprint. (with corr.) ed., 1993.

21. J. R. Graham, "Strehl ratio und marechal criterion," tech. rep., UC-Berkeley, Astronomy Department, 2006.

22. C. L. Häfner, *Entwicklung, Modellierung und Aufbau des 10 Joule-Vorverstärkers mit adaptiver Optik für den Petawatt-Laser PHELIX*. PhD thesis, Ruprechts-Karls-Universität, Heidelberg, October 2003.

23. J. H. Pitts, M. K. Kong, and M. A. Gerhard, "Thermal Stress in Edge Cladding of NOVA Glass Laser Disk," in *12th Symposium on Fusion Engineering*, **12**, IEEE, September 1987.

24. H.-M. Heuck, S. Borneis, E. W. Gaul, C. Häfner, T. Kühl, P. Wiewior, and U. Wittrock, "Waverfront Measurement and Adaptive Optics at the PHELIX Laser," in *Proceedings of the 4th International Workshop on Adaptive Optics for Industry and Medicine*, U. Wittrock, ed., pp. 283–290, Springer, Berlin Heidelberg New York, 2005.

25. J. E. Murray and F. Bonneau, "Spatial filter issues," in *3rd Annual International Conference on Solid State Lasers for Application to Inertial Confinement Fusion*, (Monterey (CA)), June 1998.

26. H.-M. Heuck, *Einsatz adaptiver Optik und Kompensation chromatischer Aberration beim Petwattlaser PHELIX*. PhD thesis, TU Clausthal, 2006.

27. C. J. Hooker, C. J. Reason, I. N. Ross, M. J. Shaw, and N. M. Tucker, "Progress in adaptive optics for laser beam phasefront control," tech. rep., CLRC Rutherford Appelton Laboratory, 1997.

28. W. Press, S. Teukolsky, W. Vetterling, and B. Flannery, *Numerical recipes in C: the art of scientific computing*, Cambridge University Press New York, NY, USA, 1992.